Earthquake Engineering, Tenth World Conference © 1992 Balkema, Rotterdam. ISBN 90 5410 060 5

Damping effects of a vibration control damper using sloshing of water

H. Kosaka, T. Noji, H. Yoshida, E. Tatsumi, H. Yamanaka & A. K. Agrawal
Mitsui Construction Co. Ltd, Japan

Abstract: This paper describes the damping effects of a vibration control system, widely known as Tuned Liquid Damper (TLD). This damper utilizes the hydrodynamic force of water. The vibration characteristics of the TLD-structure coupled system and the hydrodynamic force characteristics of the TLD were studied experimentally. The effectiveness of TLD as a vibration control system has been demonstrated. Based on the experimental results, experimental formulas for the damping factor of the TLD were developed for numerical simulation. The adequacy of this approach has been shown by numerical simulation of a single-degree-of-freedom system.

1. INTRODUCTION

The vibration control system, named Tuned Liquid Damper (TLD), has been widely recognized as an effective damper for reducing the structural vibration due to earthquake, strong wind and other dynamic loadings (Modi et al., 1987 and Fujino et al., 1988). In this damper, the sloshing period of the TLD is tuned to the fundamental period of the structure. This damper exploits the hydrodynamic force of the liquid (water) to control the vibration of the structure. The authors have proposed the frequency response analysis method using the hydrodynamic force obtained from the experiments on model water tanks and discussed the damping effects earlier also (Noji et al. 1988, 1989 and 1990). We have also investigated the damping effects of the TLD in the strong wind by applying it to a high-rise observatory tower of height 158 meters (Noji et al., 1991).

Fig. 1 shows the vibration control mechanism of the damper. The objective device consists of a rectangular water tank and wire nets (damping nets) for controlling the damping of water movement. In the present study, we first conducted a model vibration experiment to study the nature of variation of the hydrodynamic force of the TLD with the aspect ratio (water tank length/water depth) of the TLD and the number of damping nets. Then, we studied experimentally the damping in the controlled structure (TLD-structure coupled system) by changing the mass ratio of water to the structure, the aspect ratio and the number of nets. Based on the experimental results, we developed experimental formulas for the damping factor of the TLD. The adequacy of the analytical method has been shown by numerical simulation of a single-degree-of-freedom system.

2. HYDRODYNAMIC FORCE CHARACTERISTICS OF THE TLD

2.1 Steady state vibration experiment of the TLD

2.1.1 Outline of the experiment

Fig. 2 shows the experimental setup. Two water tanks of lengths 1.5 m and 3.0 m were used (assuming the lengths to be 1/1~1/5 of those in the real application).

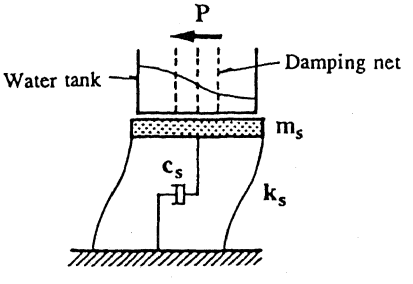

Figure 1. Vibration control mechanism of the Tuned Liquid Damper.

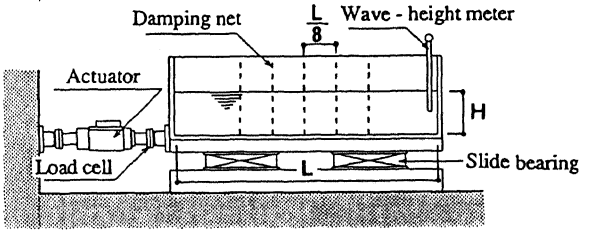

Figure 2. Experimental setup of TLD.

Six cases of aspect ratio, the ratios being in the range 4~16, were considered. Different parameters of the TLD and the natural frequency of the TLD for each aspect ratio are shown in Table 1. One, three and five damping nets with wire diameter 1.1 mm and aperture rate 51.3 % were placed such that the plane of every net was perpendicular to the direction of water motion. In case of single net, it was placed in the center of the tank. In other cases, nets were placed symmetric to the center one at the spacing of L/8, as shown in Fig. 2.

Forced vibration experiment with constant amplitude and unidirectional excitation was conducted. The non-dimensional excitation amplitude, D/L (D:excitation amplitude, L: water tank length) and the non-dimensional frequency f/f_n (f: excitation frequency, f_n: theoretical sloshing frequency) were in the range 0.0005~0.1, and 0.7~1.3 respectively. The effects of the frictional force of slide bearing and the inertia force of the water tank were obtained by conducting an experiment using sand bags whose weight was equal to the water mass. The hydrodynamic force characteristics of the liquid motion was obtained by deducting the friction and inertia force effects from the TLD experimental results.

Table 1. Parameters of TLD

L/H	4	6	8	10	12	16
L(m)	1.5	1.5	3.0	3.0	3.0	3.0
H(m)	0.375	0.250	0.375	0.300	0.250	0.188
f_n (Hz)	0.584	0.500	0.312	0.281	0.258	0.225

2.1.2 Frequency response characteristics of the hydrodynamic force

The response magnification plots of hydrodynamic force and the phase lag for aspect ratios 4 and 12 are shown in Figs. 3 and 4 respectively. Both these cases of aspect ratios have been studied by taking 1 and 3 damping nets. The horizontal axis indicates the non-dimensional frequency f/f_n. The response magnification of hydrodynamic force is obtained by dividing the amplitude of hydrodynamic force P by $Po=(2\pi f)^2 D\, m_w$ (m_w: water mass). The hydrodynamic force shows nonlinear behavior, dependent on the exciting amplitude: as the exciting amplitude becomes larger, the peak becomes smoother and the phase lag changes more gradually. This means that the damping of the TLD increases with increase in exciting amplitude. Also when the number of damping nets is increased, the peak value of the hydrodynamic force response magnification becomes smaller, meaning

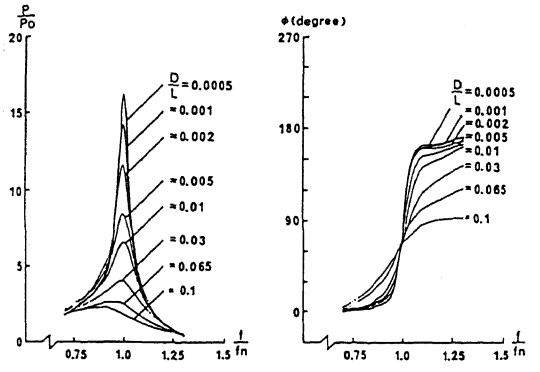

(1) N=1

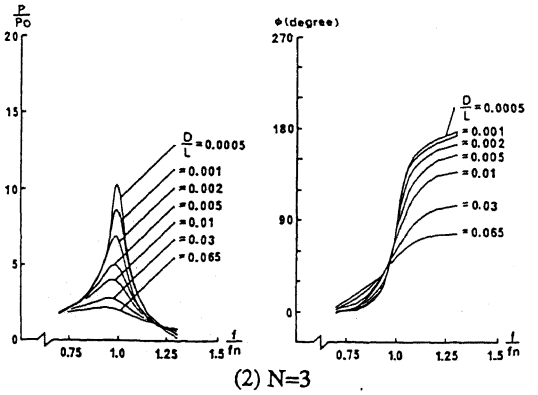

(2) N=3

Figure 3. The characteristics of hydrodynamic force (L/H = 4).

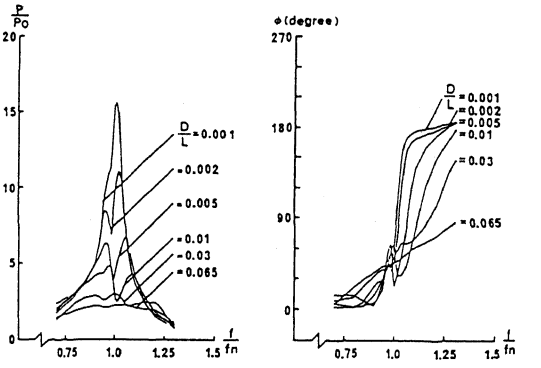

(1) N=1

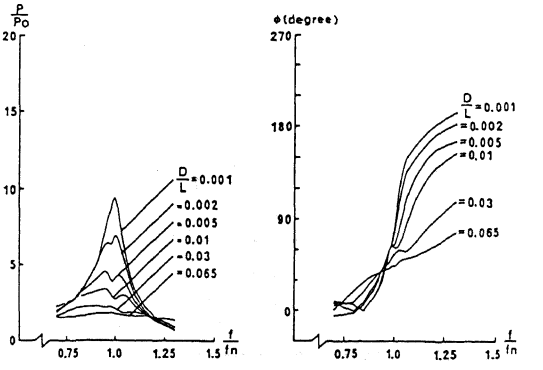

(2) N=3

Figure 4. The characteristics of hydrodynamic force (L/H = 12).

higher damping.

We also observe from these figures the effect of change of aspect ratio on the response magnification of hydrodynamic force. In case of aspect ratio 4, single sharp peak occurs at the non-dimensional frequency 1.0. However, for aspect ratio 12, the peak value of the response magnification becomes smaller and both the response magnification and the phase lag change in complicated manner with the increase in excitation amplitude. This phenomenon occurs because several types of waves are formed in the tank due to progressive waves.

The relationship between the exciting amplitude ratio, the response magnification and the damping factor h_{eq} of the hydrodynamic force are shown on log-log scale in Fig. 5. The equivalent damping factor was evaluated from the wave height and the frequency response curve of the hydrodynamic force, based on single-degree-of-freedom system model. We also observe from this figure that the peak response magnification of hydrodynamic force decreases linearly with the increase in exciting amplitude on the log-log scale. This relationship doesn't depend on the aspect ratio and a parallel relationship is observed with the number of damping nets. Also the equivalent damping factor increases linearly with the increase in exciting amplitude. Similar to the case of the peak response magnification of hydrodynamic force, this relationship doesn't depend on the aspect ratio and a parallel relationship is observed with the number of damping nets in this case also.

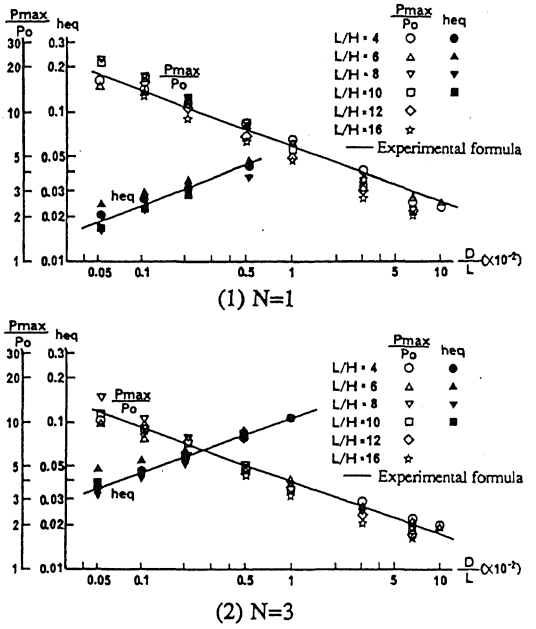

Figure 5. P_{max}/P_0 and h_{eq} versus D/L on log-log scale.

2.2 Experimental formula based on the hydrodynamic force characteristics of the TLD

A relationship between the response magnification of the hydrodynamic force and the equivalent damping factor, shown by Equations (1) and (2), was obtained by the method of least squares.

$$\frac{P_{max}}{P_0} = 1.22\beta^{-0.45}\left(\frac{D}{L}\right)^{-0.36} \quad (1)$$

$$h_{eq} = 0.30\beta^{0.57}\left(\frac{D}{L}\right)^{0.36} \quad (2)$$

where, β is a constant dependent on the location and number of damping nets and can be obtained by:

$$\beta=\sum_{i=1}^{N} \sin^2\left(\frac{\pi x_i}{L}\right) \quad (3)$$

where, x_i is horizontal coordinate of the i-th damping net. Equations (1) and (2) are shown by solid lines in Fig. 5. We observe that the powers of D/L in Equations(1) and (2) are same in magnitude and opposite in sign. From these equations, we also observe a parallel relationship between the equivalent damping factor and the number of damping nets.

3. RESPONSE CHARACTERISTICS OF TLD-STRUCTURE COUPLED SYSTEM

3.1 Outline of the experiment

3.1.1 Experimental model and parameters

The frequency response characteristics of the TLD-Structure coupled system and its behavior under random base excitation were investigated by shaking table experiment. Fig. 6 shows the experimental setup. The mass ratio m_w/m_s, aspect ratio L/H and the number of damping nets N were considered as experimental parameters. The one storey model was made of steel columns and steel floor of mass 2.0 tons. The fundamental natural frequency , f_s = 0.897 Hz and inherent damping, h_s = 0.3 % were identified by frequency response experiment with 0.1 mm exciting amplitude.

Two types of damping devices were considered: "TYPE 1" with relatively deep water depth and the aspect ratio 5.3 and "TYPE 2" with shallow water depth and the aspect ratio 13.2 as shown in Table 2. The water depth was calculated such that the sloshing frequency of water motion based on the linear wave

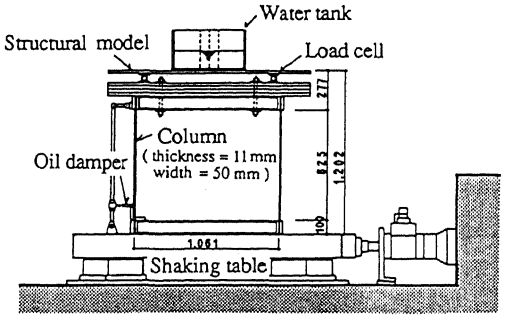

Figure 6. Experimental setup of TLD-Structure coupled model.

theory coincided with the fundamental natural frequency of the model. The mass ratio was set to 1, 2, and 4 % depending on the number of water tanks. The number of water tanks was 1 for "TYPE 1" and 29 for "TYPE 2", both corresponding to 1 % mass ratio. The number of water tanks for other mass ratios can be obtained by multiplying these numbers by the percentage of corresponding mass ratios. The experiment was conducted using both 1 and 3 damping nets.

Table 2. Parameters of TLD in TLD-Structure coupled model for 1 % mass ratio

	L (cm)	B (cm)	H (cm)	L/H	f_n (Hz)	W_w (kg)
TYPE 1	51.8	40.0	9.8	5.3	0.897	20.3
TYPE 2	22.7	18.0	1.7	13.2	0.897	0.69

3.1.2 Exciting method

The model was subjected to constant amplitude harmonic excitation in one direction. The exciting frequency f was in the range 0.7~1.1Hz and the exciting amplitude X_T was 0.1 mm and 0.6 mm. Also the model subjected to two types of random seismic excitations: EL CENTRO 1940 NS and TAFT 1952 EW. However, these base inputs were scaled down by 1/2.5 along the time axis. The input intensity level of these earthquakes was decided such that the maximum displacement of the model without TLD was approximately 10, 20, 40 and 60 mm. Table 3 shows different cases of input intensity levels of these two earthquakes.

3.2 Frequency response characteristics of the TLD-Structure coupled model

The results of frequency response experiment for mass ratio 2 % and 4 % and 3 damping nets is shown in Fig. 7. The vertical axis in the figure shows the non-dimensionalized response ratio X/X_{0max}, where X is the experimental response of the model and X_{0max} is calculated peak resonant response of the structure without TLD. It can be noted that the response ratio is influenced by the aspect ratio, damping net numbers and exciting amplitudes. From this figure, vibration control effect of TLD can be observed. For X_T = 0.6 mm, the peak response ratio is larger because the damping of the TLD is more than that of in case of X_T = 0.1 mm. This effect can be observed more clearly in the case of "TYPE 2". This is because with increase in aspect ratio, the ratio of displacement of structure to the water tank length becomes larger, making the damping of the TLD larger than the optimum damping.

3.3 Response to random seismic excitation

Fig. 8 shows the acceleration response waveform for input peak intensity 55.1 gal . The mass ratio is 2 % and the number of damping nets is 3. From this figure, we observe significant damping effect after the peak response acceleration. The Fourier spectrum of response acceleration of the structure without TLD and with TLD for different mass ratios is shown in Fig. 9. We note that with increase in mass ratio, the peak value at the natural frequency of the structure becomes smaller, which indicates significant damping effect. We

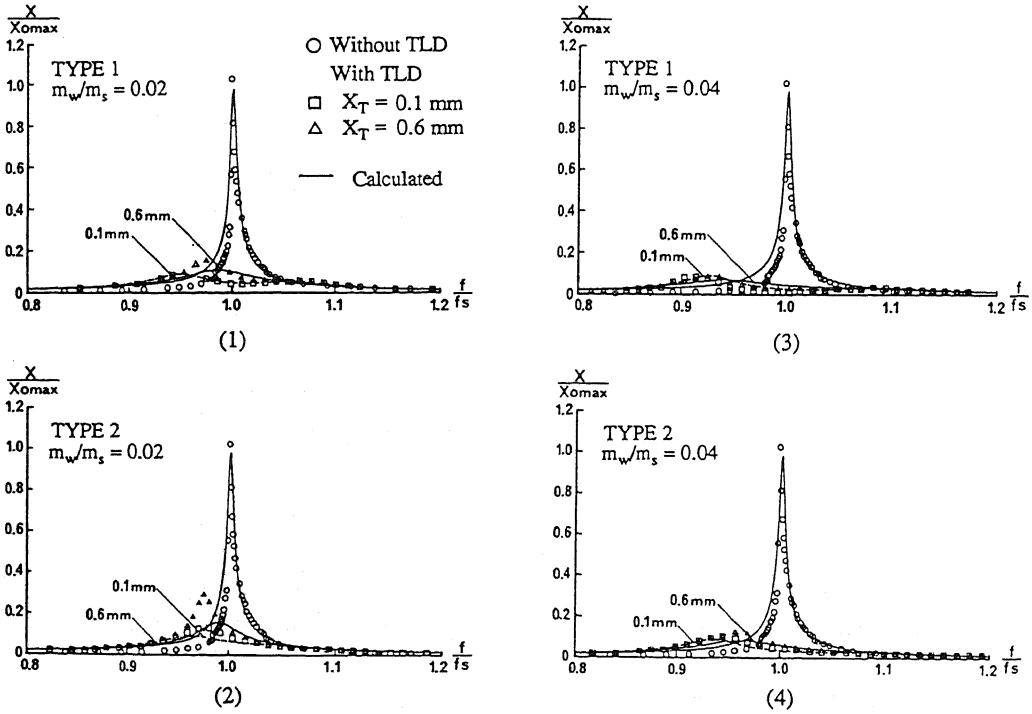

Figure 7. Frequency response curves for the TLD-Structure coupled model experiment.

also note that with larger mass ratios, two peaks are observed in the spectrum. This is because the smaller structural displacement to water tank length ratio decreases the damping of the TLD.

Figure 10 shows the maximum response acceleration ratio ($\alpha_{max}/\alpha_{0max}$) versus input acceleration intensity and the standard deviation ratio ($\sigma_{max}/\sigma_{0max}$) of acceleration waveform versus input acceleration intensity. Here, α_{max} and α_{0max} stand for maximum acceleration of the structure with and without TLD respectively and σ_{max} and σ_{0max} stand for maximum standard deviation of the structural acceleration with and without TLD respectively. The number of damping nets is 3 for all the cases of mass ratios and base inputs. The standard deviation has been calculated for the duration of 30 seconds from the beginning. We observe from these figures that the damping effect due to TLD increases with mass ratio. We also observe that with increase in mass ratio, the decrease in standard deviation is more than that of in maximum acceleration. The maximum acceleration ratio remains almost unaffected by the increase in the intensity of input base motion. However, the standard deviation increases slightly with increase in input base intensity.

Table 3. Input levels of earthquake excitation

CASE	ELCENTRO, 1940 NS		TAFT, 1952 EW	
	$\ddot{y}_{max}$(gal)	y_{max}(cm)	$\ddot{y}_{max}$(gal)	y_{max}(cm)
1	55.1	0.176	155.9	0.345
2	108.7	0.350	270.4	0.625
3	229.2	0.734	610.4	1.486
4	365.0	1.189	—	—

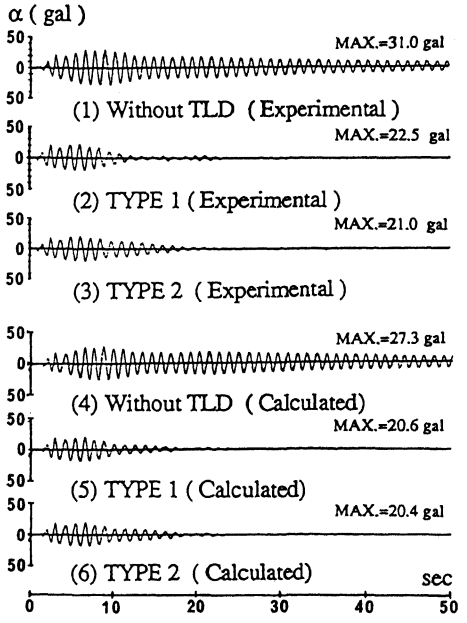

Figure 8. Response acceleration waveforms for ElCentro, 1940, NS input.

3.4 Simulation of the experimental results

A two-degree-of-freedom has been adopted for numerical simulation. Based on the Tuned Mass Damper analogy, the TLD is replaced by a SDOF mass-spring-dashpot system. The equivalent TMD mass M1 for this analogous system is calculated by Housner (1957). The ratio of M1 to the entire water mass is 0.75 for "TYPE 1" and 0.8 for "TYPE 2". The ratio of M1 to the mass of structure has been found to be 1.5 % for "TYPE 1" and 1.6 % for "TYPE 2". The damping factor h_{eq} for the equivalent TMD has been calculated for the particular amplitude of excitation from the experimental formula described in section 2.

Fig. 7 shows the frequency response curve obtained by numerical simulation. It is observed from this figure that in case of X_T=0.1mm, results of numerical simulation are in very good agreement with experimental results. However, in case of X_T=0.6mm, the damping factor of the TLD seems to be underestimated in numerical simulation. This may be because the experimental formula for h_{eq} is no longer linear on log-log scale for X_T=0.6 mm. At large excitation amplitudes, wave breaking phenomenon occurs. The damping effect due to this phenomenon is

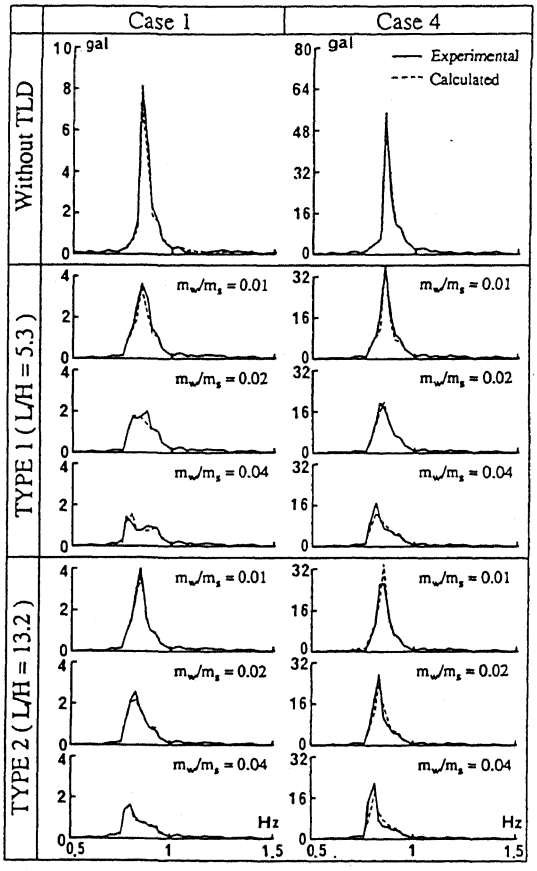

Figure 9. Fourier spectrums of response acceleration waveforms for ElCentro, 1940, NS input.

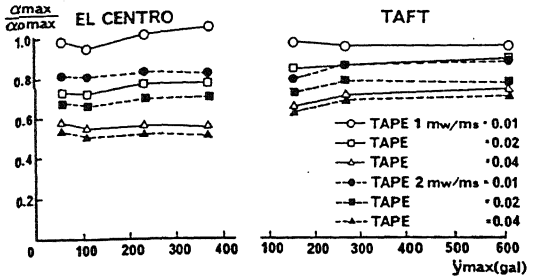

(1) Maximum response acceleration ratios.

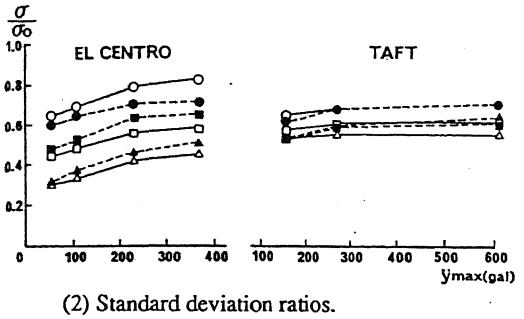

(2) Standard deviation ratios.

Figure 10. Maximum response acceleration ratios and standard deviation ratios for ElCentro, 1940, NS and Taft, 1952, EW inputs.

not accounted for in the experimental formula.
Figs.8 and 9 show the results of numerical simulation for seismic base excitation. We again observe a good agreement between experimental and simulation results. However, we note from this figures that the agreement between experimental and simulation results deteriorate slighly when the input base motion intensity increases, as shown under case 4 in Fig. 9.

From the discussion in this section, we note that the TMD analogy gives good results if h_{eq} is chosen rationally using the experimental formula.

4. CONCLUSIONS

Experiments were conducted to investigate the effect of TLD on structural vibration control capability. Based on the experimental results, a formula for equivalent damping of the TLD has been developed. Good agreement between experimental and numerical results has been demonstrated. The conclusions of this study are summarized as follows:

i) The Tuned Liquid Damper is capable of controlling the vibration of the structure effectively if the mass ratio, aspect ratio and damping nets are designed properly considering the objective external excitation.

ii) In case of seismic excitation, the damping effect is significant after the peak response has been reached. Also, the peak response value decreases with increase in mass ratio.

iii) Numerical simulation can be performed by TMD analogy. The results of simulation have been found to be in good agreement with experimental results.

ACKNOWLEDGEMENTS: We would like to express our deepest gratitude to Dr. Sadaichi Terada, professor of Tokyo Metropolitan University and Dr. Takeshi Ohkuma, professor of Kanagawa University for their invaluable comments and suggestions regarding the present study. The experiment was conducted in collaboration with Mitsui Engineering & Shipbuilding Co., Ltd. We offer our sincere gratitude to the concerned people of the company.

REFERENCES

Modi, V.J. and Welt,F. 1987. Vibration control using nutation dampers. Proc. Int. Conf. Flow Induced Vibration, England: 369-376.

Fujino, Y. et al. 1988. Parametric studies on tuned liquid damper(TLD) using circular containers by free-oscillation experiments. Struct. Engrg. / Earthq. Engrg., Proc. JSCE, No.398: 381-391.

Tamura, Y. and Fujii, K. et al. 1988. Wind-induced vibration of tall towers and practical applications of tuned sloshing damper. Proc. Sympo./Workshop on Serviceability of buildings, Canada: 228-241.

Noji, T. et al. 1988. Study on vibration control damper utilizing sloshing of water. Journal Wind Engrg., No.37, Japan: 557-566.

Noji, T. et al. 1989. Vibration control damper using sloshing of water. Struct. Design Analysis test., ASCE Struct. Cong.: 1009-1018.

Noji, T. et al. 1990. Study of water-sloshing vibration control damper (Part 1). Journal Struct. Constr. Engrg, AIJ, No.411: 97-105.

Noji, T. et al. 1991. Verification of vibration control effect in actual structure. Journal Struct. Constr. Engrg, AIJ, No.419: 145-152.

Noji, T. 1991. Vibration control of structures using sloshing of water. Doctoral Thesis. Tokyo metropolitan University, Tokyo, Japan.

Housner, G.W. 1957. Dynamic pressures on accelerated Fluid Containers. Bulletin of Seismological Society of America: 15-35.